2017

Chevrel Phase Mo6T8 (T = S, Se) as Electrodes for Advanced Energy Storage

Lin Mei
Hunan University

Jiantie Xu
University of Wollongong, jxx125@case.edu

Zengxi Wei
Hunan University

Hua-Kun Liu
University of Wollongong, hua@uow.edu.au

Yutao Li
University of Texas at Austin

See next page for additional authors

Publication Details

Mei, L., Xu, J., Wei, Z., Liu, H., Li, Y., Ma, J. & Dou, S. (2017). Chevrel Phase Mo6T8 (T = S, Se) as Electrodes for Advanced Energy Storage. Small, 13 (34), 1701441 -1-1701441 -11.

Chevrel Phase Mo6T8 (T = S, Se) as Electrodes for Advanced Energy Storage

Abstract
With the large-scale applications of electric vehicles in recent years, future batteries are required to be higher in power and possess higher energy densities, be more environmental friendly, and have longer cycling life, lower cost, and greater safety than current batteries. Therefore, to develop alternative electrode materials for advanced batteries is an important research direction. Recently, the Chevrel phase Mo 6 T 8 (T = S, Se) has attracted increasing attention as electrode candidate for advanced batteries, including monovalent (e.g., lithium and sodium) and multivalent (e.g., magnesium, zinc and aluminum) ion batteries. Benefiting from its unique open crystal structure, the Chevrel phase Mo 6 T 8 cannot only ensure rapid ion transport, but also retain the structure stability during electrochemical reactions. Although the history of the research on Mo 6 T 8 as electrodes for advanced batteries is short, there has been significant progress on the design and fabrication of Mo 6 T 8 for various advanced batteries as above mentioned. An overview of the recent progress on Mo 6 T 8 electrodes applied in advanced batteries is provided, including synthesis methods and diverse structures for Mo 6 T 8 , and electrochemical mechanism and performance of Mo 6 T 8 . Additionally, a briefly conclusion on the significant progress, obvious drawbacks, emerging challenges and some perspectives on the research of Mo 6 T 8 for advanced batteries in the near future is provided.

Disciplines
Engineering | Physical Sciences and Mathematics

Publication Details
Mei, L., Xu, J., Wei, Z., Liu, H., Li, Y., Ma, J. & Dou, S. (2017). Chevrel Phase Mo6T8 (T = S, Se) as Electrodes for Advanced Energy Storage. Small, 13 (34), 1701441 -1-1701441 -11.

Authors
Lin Mei, Jiantie Xu, Zengxi Wei, Hua-Kun Liu, Yutao Li, Jianmin Ma, and Shi Xue Dou

DOI: 10.1002/ ((please add manuscript number))
Article type: Progress Reports

Chevrel Phase Mo_6T_8 (T= S, Se) as Electrodes for Advanced Energy Storage

Lin Mei,[+] Jiantie Xu,[+] Zengxi Wei, Huakun Liu, Yutao Li, Jianmin Ma and Shixue Dou*

Dr. Lin Mei, Zengxi Wei, Prof. Jianmin Ma
School of Physics and Electronics, Hunan University, Changsha 410082, P. R. China
E-mail: nanoelechem@hnu.edu.cn (Jianmin Ma)

Dr. Jiantie Xu, Prof. Huakun Liu, Prof. Shixue Dou
Institute for Superconducting and Electronic Materials, University of Wollongong, Wollongong 2500, Australia

Dr. Y.T. Li
Materials Science and Engineering Program & Texas Materials Institute
The University of Texas at Austin, Austin , TX 78712 , USA

+These authors contribute equally.

Keywords: Mo_6S_8, Mo_6Se_8, Lithium-ion batteries, Sodium-ion batteries, Multivalent ion batteries

ABSTRACT

With the large-scale applications of electric vehicles in recent years, it requires future batteries with higher power and energy densities, longer cycling life, lower cost, more environmental friendliness and higher safety than that we have used. Under this regard, to develop alternative electrode materials for advanced batteries is an important research direction.. Recently, the *Chevrel* phase Mo_6T_8 (T= S, Se) have attracted increasing attention as electrode candidates for advanced batteries, including monovalent (*e.g.*, lithium and sodium) and multivalent (*e.g.*, magnesium, zinc and aluminum) ion batteries. Benefiting from its unique open crystal structure, the *Chevrel*

phase Mo_6T_8 can not only ensure ion transport rapidly, but also retain the structure stability during electrochemical reactions. Although the history of the research on Mo_6T_8 as electrodes for advanced batteries is short, there has been significant progress on the design and fabrication of Mo_6T_8 for various advanced batteries as above mentioned. In this **Progress Reports**, we mainly overview recent progress on Mo_6T_8 electrodes applied in advanced batteries, including synthesis methods and diverse structures for Mo_6T_8, and electrochemical mechanism and performance of Mo_6T_8. . In addition, we also briefly conclude the significant progress, obvious drawbacks, emerging challenges and some perspectives on the research of Mo_6T_8 for advanced batteries in the near future.

1. Introduction

The development of advanced and renewable energy storage devices has raised great concerns due to the rapid depletion of fossil fuels and ever-growing demand of human being over the past decades. As one of the most successful energy storage systems, rechargeable lithium-ion batteries (LIBs) have been widely utilized in portable and smart electronic devices due to their high energy densities, long cycling life and environmental friendliness.[1] However, limit natural sources of lithium, low power density and the safety issue of LIBs relatively restrict LIBs in the large scale applications of future electric vehicles (EVs). Apart from the continuous development of high performance LIBs, many efforts have been also devoted to develop alternative and promising batteries instead of LIBs, including metal-ion batteries (*e.g.*, sodium-ion batteries (SIBs) and magnesium-ion batteries (MIBs)),[2] aqueous electrolyte batteries (*e.g.*,zinc-ion batteries (ZIBs) and aluminum-ion batteries (AIBs)),[3] and hybrid batteries.[4] It is well known that the electrochemical performance of batteries highly depends on the properties of electrode materials. As expected, to search ideal electrode materials for advanced batteries is a key to the success of development of high-performance batteries.[5] The electrochemical mechanisms of the electrode materials during the charge-discharge process can be mainly divided into three types of intercalation, alloying, and conversion reactions. So

far, intercalation-type electrode materials have been successfully commercialized and still intensively investigated in rechargeable batteries.[6] Intercalation mechanism is based on the reversible insertion/extraction of metal ion (*e.g.*, alkali) into the lattice of a host structure at various potentials. During the metal ions insertion/extraction process, the host structure almost remains unchanged or is only slightly altered. Moreover, there is a few side reactions occurred at the intercalation-type electrodes during the charge-discharge processes.

As the most successfully commercialized intercalation-type materials for LIBs, graphite with low specific capacity and poor rate capability is difficult to meet the high requirement of EVs in terms of high power densities in the future. Over the past decades, there are a large number of intercalation-type materials have been explored to replace graphite for LIBs, such as β-FeOOH, α-MnO_2, MoS_2, V_2O_5, $Li_4Ti_5O_{12}$ and Mo_6T_8, due to their high theoretical capacity and stable structures.[7] Among them, *Chevrel* phase Mo_6T_8 (T = S, Se or their combination) is a kind of promising intercalation-type electrode materials, which can accommodate monovalent or multivalent ions within the Mo_6T_8 framework.[2d, 8] Since the *Chevrel* phase molybdenum chalcogenides were first reported in 1971,[9] they have been demonstrated to have strong intercalation ability and electrochemical kinetics with various multivalent ions, such as Zn^{2+}, Mg^{2+}, Mn^{2+}, Co^{2+}, Fe^{2+} and Al^{3+}.[10] The strong electrochemical kinetics of such kinds of materials was attributed to their unusual open and rigid framework that provides numerous vacant sites, short ion transporting path, and the charge-unbalance caused by bivalent ions. Typically, Aurbach *et al.*[11] for the first time found that the *Chevrel* phase Mo_6S_8 as cathode for MIBs can be charged and discharged over 2000 cycles with a capacity decay of <15%. Despite only an average working voltage of ~ 1.2 V *vs*. Mg^{2+}/Mg and a maximum reversible capacity of 130 mA h g^{-1} were obtained, the impressive cycling life of the cell still spurred intensive and further research interest on it for advanced batteries.

Moreover, the development of Mo_6T_8 for MIBs have also triggered ever-growing attention for their applications in other advanced energy storage systems (*e.g.*, LIBs, SIBs, ZIBs and AIBs), though the electrochemical study of monovalent ion (*i.e.*, Na)

intercalation/de intercalation behavior in *Chevrel* phase structure studied by Gocke *et al*. and Tarascon*et al.* can be early back to 1980s.[12] Recently, there have been an increasing number of literatures reported on the Mo_6T_8 family for energy storage systems, further indicating the research importance of Mo_6S_8 electrode materials. In this report, we mainly overview recent progress on the electrochemical energy storage applications of *Chevrel* phase Mo_6T_8, focusing on the synthesis methods, intercalation mechanism and various structure-function of Mo_6T_8, as well as their applications in various advanced batteries. In addition, we also briefly conclude the significant progress, obvious drawbacks, emerging challenges and some perspectives on the research of Mo_6S_8 for advanced batteries in the near future.

2. Mechanism of cation insertion into *Chevrel* phase Mo_6S_8

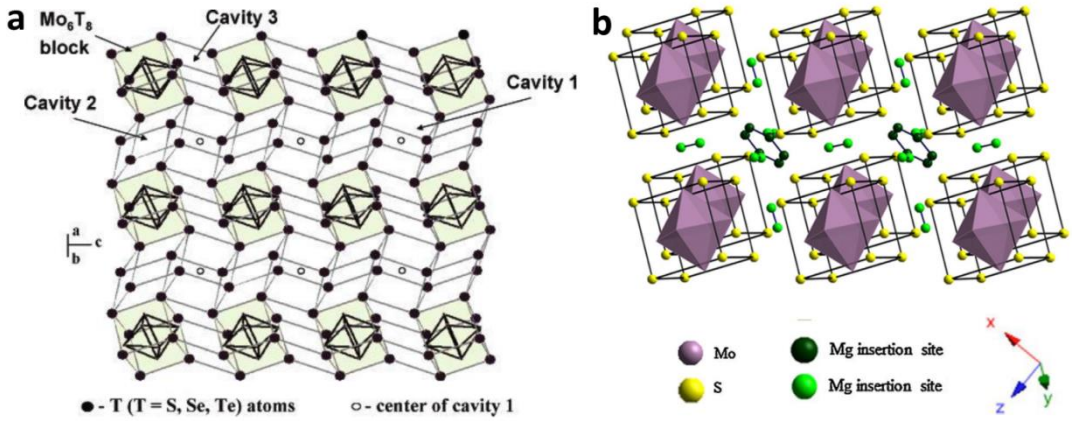

Figure 1 Different schematic presentation of crystallo graphic structure of (a) Mo_6T_8 and (b) Mo_6S_8 (a) Reproduced with permission.[10c] Copyright 2006, American Chemical Society.(b) Reproduced with permission.[8a] Copyright 2015, Elsevier.

Figure 1 displays the *Chevrel* phase Mo_6T_8 with a three-dimensional (3D) array of Mo_6T_8 units in which each Mo_6T_8 unit is composed of the octahedral cluster of molybdenum atoms inside the anion cube to form tri-directional channels for metal (M) cations [8a, 10c] As can be seen, there are three different cation locations for Mo_6T_8 (cavities 1, 2 and 3, **Figure 1a**). Cavity 1 is the site far away from Mo atom and share corner with the Mo_6T_8 cube. Cavity 2 and 3 share the edges and faces with Mo_6T_8,

respectively. Only the cavities 1 and 2 can be filled by metal cation when cavity 3 is blocked by a strong repulsion of the Mo atoms.

The location of metal cation in the cavities 1 or 2 largely depends on the size of M. The M cation with larger atomic size often locates on the center of cavities.[10c] The cation position in crystal structure of Mo_6T_8 can also be described in **Figure 1b**. As can be seen, cation (*i.e.*, Mg^{2+}) insertion into Mo_6T_8 (*i.e.*, T = S) firstly occupies the inner six sites in cavity 1 with an inner ring and the cation occupies in cavity 2 with another six sites with an outer ring, also called a quasioctahedral arrangement. Cation site on cavity 1 has lower potential energy than insertion cavity 2. As expected, intercalation into site 1 to form $MgMo_6S_8$ occurs before intercalation into site 2 and thus a trace amount of charges will be easily trapped within site 1 rather than site 2. However, it is evidenced that charge trapping of Mo_6S_8 in site 1 can be reduced through the substitution of S by selenium (Se).[13] This is due to the substitution resulting a triclinic distortion to the crystal structure with a lower activation barrier, and thereby facilitating the migration of Mg. In addition, the Se ions with larger atomic size than S slightly increased the lattice constants of intercalation compounds, which could also promote the cation mobility. Based on the crystal structure of *Chevrel* phase, several different monovalent (*e.g.*, Li, Na) and multivalent cations (*e.g.*, Zn, Mg, Al) as insertion type batteries have been studied

3. Synthesis of *Chevrel* phase Mo_6T_8

Typically, the preparation of Mo_6T_8 using $M_xMo_6T_8$ (M=Metal, T=S, Se) as the precursor can be classified into two mostly common categories: *i.e.*, high-temperature (1100-1200 ^oC) solid state reactions method with mixing elements in a quartz ampule [10f, 14] and molten salt method conducted at ~850 ^oC.[15] Both approaches require chemical leaching of the metal from the *Chevrel* phase $M_xMo_6T_8$ to completely remove metal and then obtain stable Mo_6T_8. The particle size of Mo_6T_8 synthesized by above methods was mostly in micrometer-scale and irregular shape. Developing the method with simple approach is still challenging. To obtain a high purity and uniform nanometer of Mo_6T_8, a number of several novel synthesized approaches have

been developed.[16]

Initially, $M_xMo_6T_8$ are synthesized through a solid state method by blending elemental metal, molybdenum, and sulfur powders and then transferred to heat at high temperature of 1000-1200 ^oC. In the following leaching process, although the structural integrity of $M_xMo_6T_8$ after the removal of metal can be easily preserved, the electrochemical performance of Mo_6T_8 highly depends on the leaching condition and the purity of compounds. The utilization of oxidants in chemical leaching should avoid the side reaction when various oxidants are commonly used, such as HCl, I_2, or NO_2BF_4.[17] In order to develop feasible leaching method for the high purity of Mo_6T_8, Lancry *et al.*[14a] optimized leaching conditions for M_xMo_6. First of all, the $Cu_2Mo_6S_8$ was prepared through the reaction of the powdered elements mixture. Then, three different oxidants was used: (i) 6 M HCl in water, (ii) 0.2 M I_2 in acetonitrile (AN) and (iii) 0.05 M NO_2BF_4 in AN. The chemical leaching experiences two phase-transition steps (*i.e.*, $Cu_2Mo_6S_8 \rightarrow CuMo_6S_8 \rightarrow Mo_6S_8$). Based on the quantitative X-ray diffraction (XRD) analysis on the electrode, the leaching process at the first step occurs very easily and the second step happens much slower. Owing to the use of different oxidizers, the crystallinity of Mo_6S_8 is different. The XRD intensity for the products leached by HCl/H_2O and I_2/AN were quite similar but much smaller for that by NO_2BF_4/AN. According to the electrochemical test of Mo_6S_8 for MIBs, $Cu_2Mo_6S_8$ chemically leached by I_2/AN or by HCl/H_2O is able to deliver the high discharge capacity (close to theoretical capacity) in the initial cycle. Unlike I_2/AN or HCl/H_2O, the stronger oxidizer of NO_2BF_4/AN results in the oxidation of Mo and S atoms on the surface of Mo_6S_8, which limit the electrode activity and capacity.

The preparation of $M_xMo_6T_8$ by solid state reaction often requires high temperature treatment of the samples for several days. As expected, the long time in total of synthesis of Mo_6T_8 (include chemical leaching process) is a critical issue. Recently, Gershinsky *et al.* [16a] developed a fast self-propagating high-temperature synthesis (SHS) method to prepare *Chevrel* phase $M_xMo_6T_8$. The synthesis process is very fast and its synthesis duration is only a few seconds or minutes. It is attributed to

a self-sustaining highly exothermic reaction leading to a combustion wave and thermal explosion. It should be noted that the yield of material from SHS method is also high (*e.g.*, 96 wt.% $Cu_2Mo_6S_8$). In spite of the low duration of synthesis of $M_xMo_6T_8$, the synthesis temperatures of SHS method reached extremely high up to 4000K, which could improve total cost of energy consumption.

Compared to solid state reactions and SHS approach at high temperature, molten salt synthesis and solution chemistry method are great alternatives to control the size and homogeneity of $M_xMo_6T_8$ at relative low temperature. By using molten salt synthesis method, Ryu *et al.* [15c] prepared a series of Mo_6S_8 with various particle sizes as a function of different ratios of salt to precursor. The particle size of Mo_6S_8 decreased from 0.75 to 0.24 μm with the increase on the ratio of salt (KCl)/precursor from 2 to 4. Benefiting from the reduced ion diffusion path, the electrochemical properties were improved by decreased particle size of Mo_6S_8 for MIBs. Nevertheless, Mo_6S_8 with a particle size of 0.57 μm (6/1) displayed the best electrochemical performance among the series. Therefore, to find an optimized ratio of salt: precursor for the synthesis of Mo_6S_8 is important. Moreover, Saha *et al.* [16c] reported a Mo_6S_8 with cuboidal shaped structure, which was developed from the precursor of $Cu(NH_4)_qMo_3S_9$ mainly includes two steps: (i) heat-treatment of $Cu(NH_4)_qMo_3S_9$ at 1273 K for 5 h under a gas mixture of H_2/Ar to directly yields $Cu_2Mo_6S_8$ and (ii) removal of copper from $Cu_2Mo_6S_8$to form Mo_6S_8 using hydrochloric acid treatment. Both the $Cu_2Mo_6S_8$ and Mo_6S_8 are unique cuboidal shaped particles in the 1-1.5μm size, which displayed the encouraging electrochemical performance.

To get the uniform particle distribution and reduce particle size of Mo_6T_8, which is beneficial for Mo_6T_8 with the improved electrochemical performance, there are also several approaches (*e.g.*, microwave route and graphene-assisted method) to synthesize $M_xMo_6T_8$. Cheng *et al.*[16e] reported a facile method to obtain $Cu_2Mo_6S_8$ nanocubes by a graphene-assisted approach. The utilization of graphene in the solution processing is beneficial to form $Cu_2Mo_6S_8$ with smaller particle size (20-150 nm) and more uniform particle distribution than that without graphene (micrometric scale). This is arise from that graphene provides a good platform for heterogeneous

nucleation and growth of particles, leading to high-quality $Cu_2Mo_6S_8$ nanocubes with well-defined phase and structures, as shown in **Figure 2**. Murgia *et al.*[16d] developed a cost-effective solid-state microwave-assisted method to effectively replace the heat process of M_xMoS_8 (*i.e.*, $Cu_2Mo_6S_8$) at high temperature. In addition, the $Cu_2Mo_6S_8$ can be obtained in a short time of ~ 400s and format the cuboidal microscale particles (0.5-2 μm).

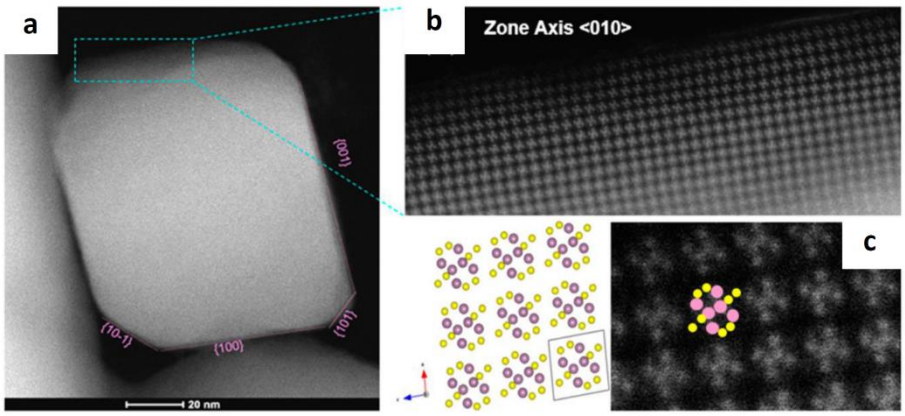

Figure 2. (a) High-angle annular dark field-scanning transmission electron microscope (STEM-HAADF) image of a single cubic Mo_6S_8 particle.(b) Atomic scale STEM-HAADF image of selected area from (a). (c) Schematic crystal structure and corresponding STEM image of Mo_6S_8 phase (Purple: Mo and yellow: S atoms). [16e] Reproduced with permission. Copyright 2016, American Chemical Society

4. Mo_6S_8 for Monovalent (Li, Na) ion rechargeable batteries

4.1 Mo_6S_8 for LIBs

Mo_6S_8 have been studied as anode material for high-rate LIBs mainly because of its considerable theoretical capacity and high electronic/ionic conductivity. Nagao *et al.* carried out a series of research works using Mo_6S_8 as an electrode material.[18] Firstly, the $Cu_xMo_6S_{8-y}$ electrode at room temperature showed excellent cycling stability with a constant reversible capacity of 100 mA h g^{-1} for 2000 cycles at a current density of 1.28 mA cm^{-2} (2 C). Moreover, the Li-In/ $Cu_xMo_6S_{8-y}$ cell with the use of Li_2S-P_2S_5 solid electrolyte assembled in the all-solid-state device was measured at various temperatures from -30 to 160 ºC. At a high operating temperature of 120 ºC, the all-solid-state cell retained good charge/discharge performance at a high rate of 20 C. However, it was found that the Cu of $Cu_xMo_6S_{8-y}$ was diffused into the solid state

electrolyte, which resulted in performance degradation. After cycling charge/discharge test, a resistance layer was also observed at the interlayer between $Cu_xMo_6S_{8-y}$ electrode and electrolyte. To improve the high rate and stability performance of solid-state cells, conductive additive of acetylene black (AB) was added in solid electrolyte because of the efficient prevention of Cu diffusion. As expected, the cell at a temperature of 160 ºC retained a reversible capacity of up to 190 mA h g^{-1} at 60 C.

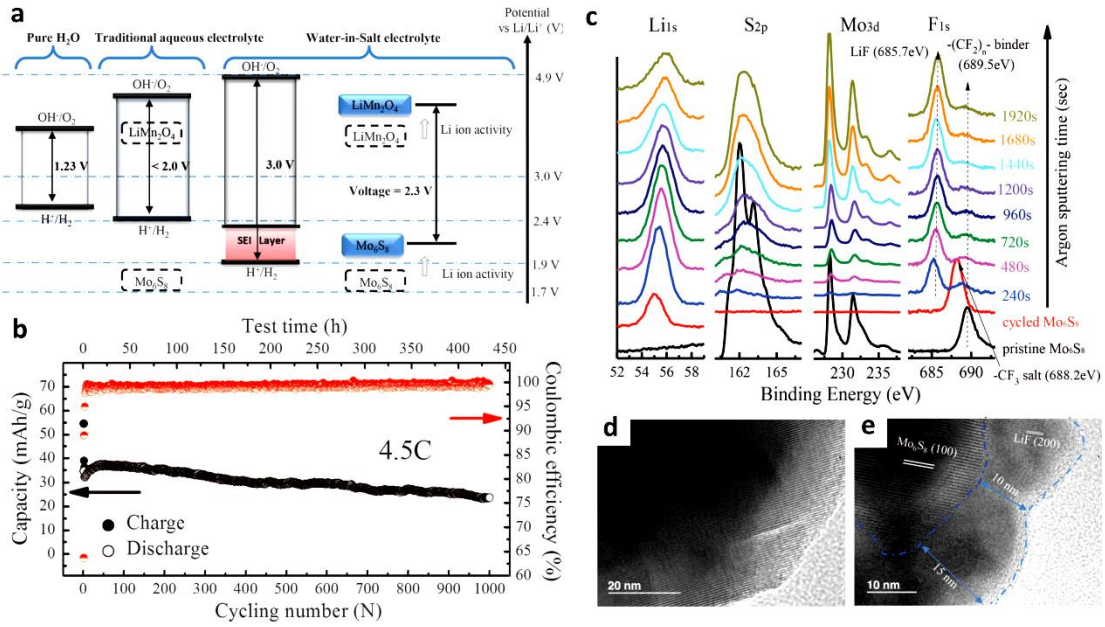

Figure 3. (a) Schematic presentation of expanded electrochemical stability window of a LIB consisting of $LiMn_2O_4$ cathode and Mo_6S_8 anode in high concentration "water-in-salt" electrolyte.(b) Cycling performance at 4.5 C of a LIB using in 21 m LiTFSI solution. (c) XPS spectra of pristine and cycled Mo_6S_8 at a full lithiation state after various durations of Ar^+ sputtering. TEM images of Mo_6S_8 before (d) and cycling (e). Reproduced with permission.[3b] Copyright 2015, AAAS

Wang *et al.* [3b] also reported a full LIBs cell consisting of "water in salt" electrolyte between Mo_6S_8 anode and a $LiMn_2O_4$ cathode. The "water in salt" electrolyte was prepared by dissolving lithium is (trifluoromethane sulfonyl) imide (LiTFSI) in water with various concentrations. As shown the **Figure 3a**, the electrochemical stability window of the fabricated cell can be expanded by the "water in salt" electrolyte. The expandable range, as well as electrochemical behavior, highly depends on the concentration of the electrolyte. For example, there is only a single redox peak at ~2.5 V for Mo_6S_8 was observed using 5 M salt electrolyte solution. When LiTFSI

concentration reached ⩾ 10 M, the second redox peak at ~2.3 V appeared. The second lithiation/delithiation happened at Mo_6S_8 anode to positive potentials was belonged to the lithium-ion activity change in the high concentration electrolyte solution. The second lithiation/delithiation process expanded the electrochemical stability window of water in salt electrolyte and completely utilized the lithium site in Mo_6S_8 electrode, otherwise inaccessible in diluted aqueous solutions. As expected, the electrochemical stability window with a high concentration electrolyte enable a full $LiMn_2O_4$ /Mo_6S_8 cell with a high output voltage, leading to an improved capacity and energy density. The fabricated full cell exhibited a high discharge capacity of 47 mA h g^{-1} (total electrode mass) and good cycling stability for 1000 cycles (**Figure 3b**). Such good electrochemical performance was attributed to a dense LiF-interphase on Mo_6S_8 surface arising from $TFSI^-$ reduction, which effectively avoid the side reactions of hydrogen evolution and oxygen reduction at an expand able electrochemical window. The existence of dense interphase was evidenced by X-ray photoelectron spectroscopy (XPS) and transmission electron microscopy (TEM) of the Mo_6S_8 before and after cycling (**Figure 3c and d**). Moreover, Wang *et al.*[19] further investigated that the "water-in-salt" electrolytes with $LiCoO_2$ as cathode when the Mo_6S_8 was still used as anode. At a current density of 0.5 C, the $LiCoO_2$/Mo_6S_8 full cell using an electrolyte of 21 M LiTFSI-0.1 wt% TMSB displays an remarkable energy density of 120 Wh kg^{-1}.

4.2 Mo_6S_8 for SIBs

Sodium-ion batteris (SIB) could be an ideal alternative to LIBs in the future due to the abundant on earth, low cost and chemically stable.[20] Extensive research has been focus on LIBs anode for high energy density, high columbic efficiency and long cycling stability, however, ideal anodes for SIBs are still limited. Moreover, developing stable capacity and high Coulombic efficiency of SIBs anode is still challenging. Compared to the metal oxide materials, Chevrel phase Mo_6T_8 have been also considered as candidate electrode for SIBs because of its unique open framework and high electronic conductivity. Saha et al.[21] for the first time studied the sodium storage properties of *Chevrel* phase cuboidal Mo_6S_8 and Mo_6Se_8, which was prepared

by a method combining two-step solution chemistry and high energy mechanical milling (HEMM). The electrochemical test revealed that electrochemical sodiation of Mo_6T_8 has two stage reactions (plateaus) ($Mo_6Se_8 \rightarrow Na_{\sim 1}Mo_6Se_8 \rightarrow Na_{\sim 3.3}Mo_6Se_8$ and $Mo_6S_8 \rightarrow Na_{\sim 1}Mo_6S_8 \rightarrow Na_{\sim 3.7}Mo_6S_8$), as shown in **Figure 4a-b**. Mo_6S_8 displayed a reversible capacity of 60 mA h g^{-1} after 50 cycles with a low capacity decay of 0.7% per cycle (**Figure 4c**) while Mo_6Se_8 achieved a low but stable capacity of 35 mA h g^{-1} after 20 cycles. The different of sodiation phases (capacity), as well as cycling stability are most likely attributed to the larger molecular weight of Se than S.

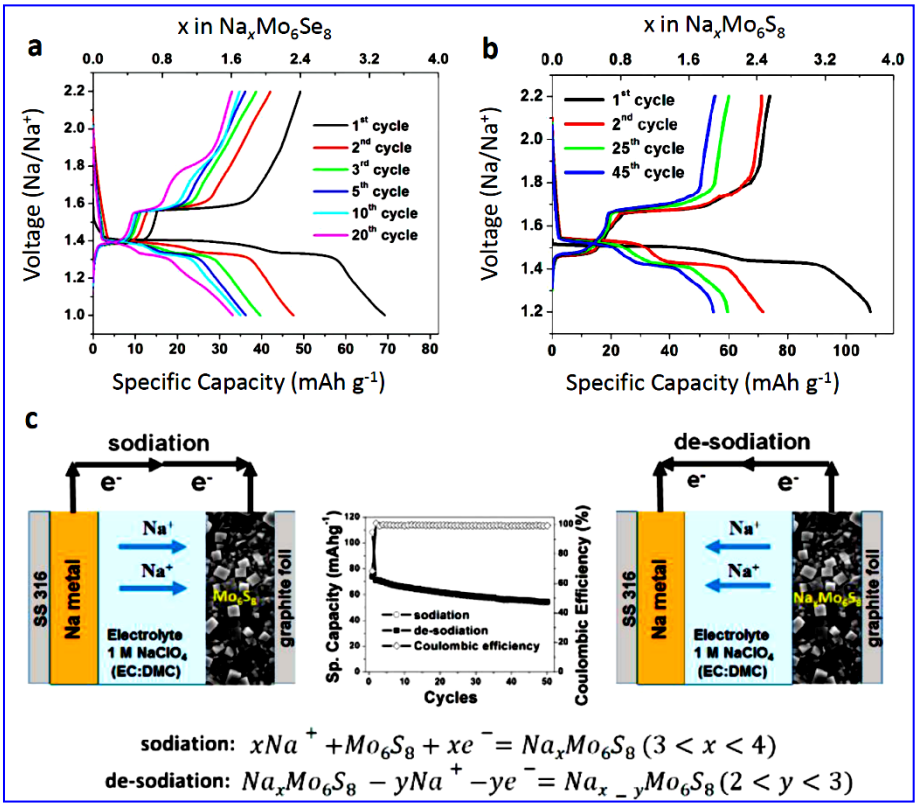

Figure 4. Discharge-charge profiles of (a) Mo_6Se_8 and Mo_6S_8 electrode at a current density of ~20 mA g^{-1} in the voltage range of 1.2-2.2V. (c) Cycling performance and a sodiation / de-sodiation mechanism of Mo_6S_8.[21] Reproduced with permission. Copyright 2015, American Chemical Society.

5. Mo_6S_8 for multivalent-ion rechargeable batteries

The mechanism of rechargeable multivalent ion batteries is similar to the monovalent alkaline ion (Li^+, Na^+) batteries.[22] It should be noted that, different from alkaline ion batteries, MIBs, ZIBs or AIBs have their own advantages, including abundance on earth, energy density and safety issues. Moreover, multivalent ion

batteries can potentially obtain higher capacity than LIBs/SIBs due to the fact that multivalent ion (*i.e.*, Mg, Zn, and Al) have various valence electrons more than lithium with only one (ion), and low molecular weight of Mg, Zn, and Al. Furthermore, the less safety issue is associated with the use of Mg, Zn, and Al metal as electrode, which has much lower risk of anode dendrite than LIBs/SIBs using unsteady metal-related anodes. Nevertheless, there are also obvious disadvantages in the development of each multivalent ion battery should be overcome. In the following, we individually summarize the recent progress on the promising *Chevrel* phase Mo_6T_8 as electrode for multivalent energy storage..

5.1 Mo_6S_8 for Mg-ion batteries

Mg-based batteries were early proposed in 1990s, and magnesium ion rechargeable cell was reported by Aurbach *et al.* in 2000,[11] based on a *Chevrel*-type Mo_6S_8 cathode/Mg metal anode with a magnesium organohaloaluminate/THF electrolyte. The fabricated MIBs delivered a reversible energy density 110 mA h g^{-1} and operated at relatively low voltage (~ 1.2V). After that, there are many efforts have been devoted to optimize the elctrochemical performance of the MIBs.[23] One of them is to improve the performance of the cathodes for MIBs. Among various candidates for MIBs, *Chevrel* phase Mo_6T_8 with the advantageous structures is a promising cathode candidate, however, how to improve the energy density of Mo_6T_8 remain challenges. So far, there have been several approaches developed to improve its energy density, mainly including i) control the particle size, ii) substitution of S with Se, and iii) incorporating metal ion(*e.g.*, Cu) into the host CP.

The decrease in particle size of the electrode materials could result the shorten diffusion paths of ions within electrode materials, high surface area for ions storage and more contacts between electrode and electrolyte. Recently, a series of Mo_6T_8 with nanosize were obtained by optimized synthesis method. For example, Aurbach *et al.*[14b] prepared and compared the electrochemical performance between the nano- and micro-scale of Mo_6T_8 in MIBs. The nanoscale particle size could improve the electrochemical kinetic of $Mo_6T_8$and shorten the ion diffusion length of Mg^{2+}. As expected, the Mo_6T_8 with nanoscale has the higher capacity than that of

microstructure. Ryu *et al.*[10c] manipulated the particle size of Mo_6T_8 by controlling the ratio of salt-to-precursor (the slat: KCl and precursor: CuS/Mo/MoS_2). As a result, the Mo_6S_8 prepared with an optimized ratio of precursor displayed a high reversible capacity of 83.9 mA h g^{-1} at a current density of 0.2 C.

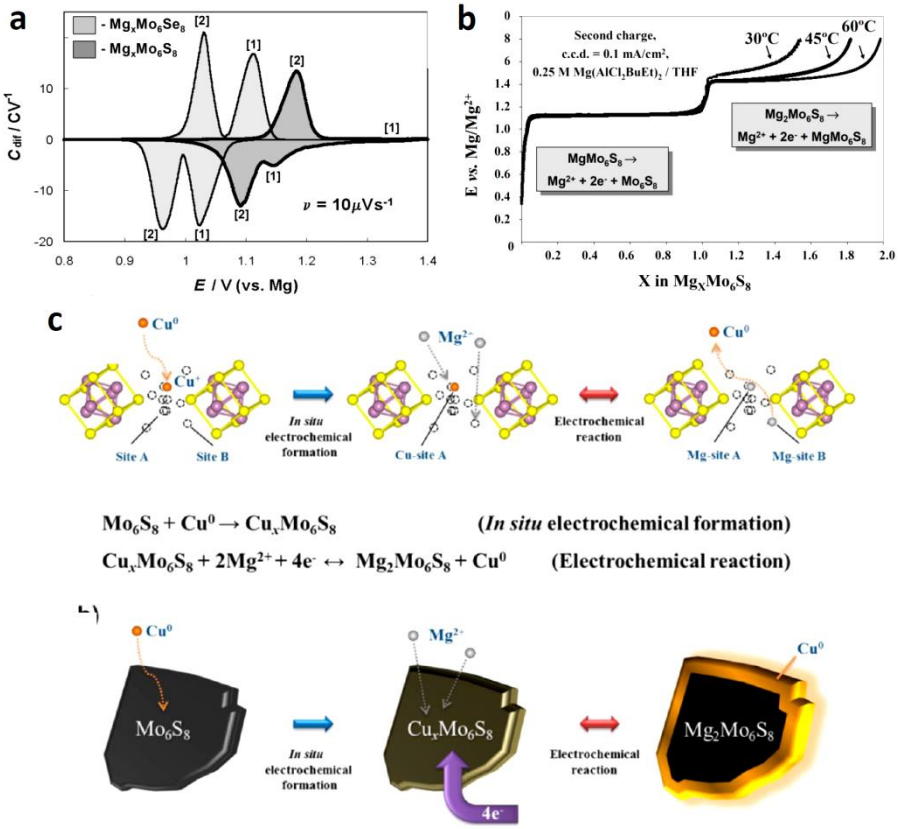

Figure 5. CV curves of Mo_6S_8 and Mo_6Se_8 as cathodes for MIBs. (b) Chronopotentiograms (V-t) curves Mo_6S_8 at various temperatures. (c) Schematic illustration of (a) Cu replacement reaction in the Mo_6S_8 during the process of Mg^{2+}insertion and extraction. (a, b) Reproduced with permission.[24] Copyright 2007, The Electrochemical Society. (c) Reproduced with permission. [14e] Copyright 2015, American Chemical Society.

Mitelman *et al.*[24] investigated Mg^{2+} transport within Mg_xMoT_6 (T= S and Se) structure and proposed a trapping mechanism. They found electrochemical kinetics (*e.g.*, Mg diffusion) of Mo_6T_8 (T= S and Se) largely depended on composition (S or Se) and working temperature of the cell (**Figure 5a**). For example, the intercalation process of Mg_xMoSe_6 is fully reversible (from x =2 *to* x =1) with excellent Mg mobility at room temperature, while partial Mg trapping (~ 25%) within Mg_xMoS_6 occurs at room temperature or even elevated temperatures (**Figure 5b**). As above mentioned, charge trapping in site 1 (**Figure 1b**) or within $MgMo_6S_8$ was significantly

reduced when substituting selenium for sulfur in the *Chevrel* Phase of $Mg_2Mo_6S_8$. This is due to the substitution of Se selenium distorting the crystal structure with high increased the lattice and lower activation barrier, which facilitates the migration of cation from insertion site 1 and thus leading to enhanced electrochemical performance. For the study on the ion intercalation mechanism, Aurbach *et al.*[25] reported that the residual Cu left from the extraction of $Cu_xMo_6S_8$ by leaching process was beneficial to improve the reversible capacity of MoS_8, during the Mg^{2+} insertion/extraction process. Woo *et al.*[14c] also found that the enhanced capacity of MoS_8 was achieved by the addition of Cu to $Cu_xMo_6S_8$ ($x > 1$). Very recently, in order to clarify the role of Cu incorporation to Mo_6T_8, Choi *et al.*[14e] investigated structural changes of the Mo_6S_8 in corporation with the Cu nanoparticle/graphene during the process of Mg^{2+} insertion and extraction. The Mo_6S_8 containing Cu nanoparticle/graphene composite is synthesized by solid state method, followed by a plasma treatment at high temperature. The results revealed that the additional capacity for $Cu_xMo_6S_8$ was attributed to the deposition/dissolution of Cu on the surfaces of Mo_6S_8 during the process of Mg^{2+} insertion and extraction **(Figure 5c)**, as evidenced by an additional reversible plateau at around 0.75 V *vs.* Mg/Mg^{2+} and the change of Mo_6S_8 morphology.

5.2 Mo_6S_8 for Zn-ion batteries

Due to low cost, abundance, environmental friendliness and high energy density (820 mA h g^{-1}) of Zinic, there are various types of batteries have been designed with a zinc metal anode.[26] So far, there is a few available host compounds that effectively accommodate Zn^{2+} with large atomic size during the charge-discharge process. As expected, the *Chevrel* phase Mo_6T_8 with open frameworks is a good candidate. The use of Mo_6T_8 as electrodes for ZIBs was recognized based on the phase transformation of ($Mo_6S_8 \leftrightarrow ZnMo_6S_8 \leftrightarrow Zn_2Mo_6S_8$) as confirmed by the galvanostatic experiments and structural analysis.[10f, 12, 16e, 27] As shown in **Figure 6a-b**, the Mo_6S_8 prepared by a solid state method delivered a discharge capacity of 134 mA h g^{-1} at a 0.05 C, with a two-plateaus discharge/charge profile.[10f] The detailed structure

changes of the Mo_6S_8 was further evidenced by *ex-situ* XRD measurements (**Figure 6c**). Recently, Cheng *et al*.[16e] employed the graphene-assisted method to synthesize the *Chevrel* phase Mo_6S_8 nanocubes and studied their electrochemical performance for ZIBs. It was found that the Mo_6S_8 can host Zn^{2+} ions reversibly in both aqueous (water) and nonaqueous 1.0 M $Zn(ClO_4)_2$ in acetonitrile or 0.4 M all-phenylcomplex (APC) dissolved in tetrahydorfuran (THF) as the electrolyte. As a result, the Mo_6S_8 nanocubes exhibited a high reversible specific capacity of ~100 mA h g^{-1}. Together with zinc-polyiodide (I^-/I_3^-)–based catholyte and zinc-polyiodide (I^-/I_3^-)-based catholytes (1.5 M ZnI_2 and 0.2 M I_2 dissolved in water) and 1.1 M $ZnSO_4$ aqueous solution as the electrolyte, the Mo_6S_8 enable the full cell demonstrating excellent cycling stability with a capacity retention of more than 90% after 350 cycles.

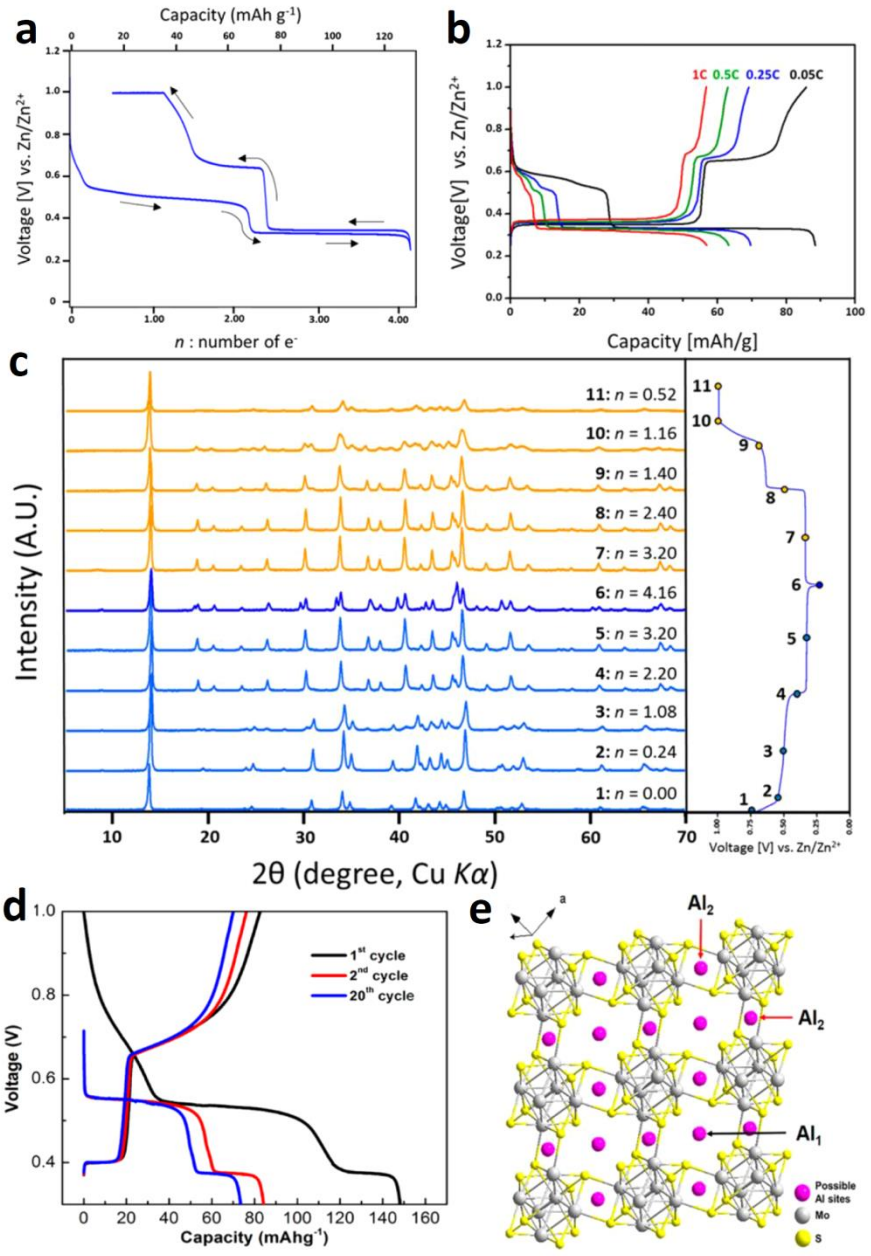

Figure 6. (a) Initial discharge-charge curves of the Zn/Mo_6S_8 cell measured at 0.05C (6.4 mA g^{-1}) and (b) various C-rates in the voltage range of 0.25−1.0 V *vs.* Zn. (c) *Ex-situ* XRD patterns of the $Zn_xMo_6S_8$ electrode at different voltage steps (d) Discharge-charge profiles of Mo_6S_8 as cathode for AIBs at 1st, 2nd, and 20th cycles and (e) crystal structure of Al intercalated Mo_6S_8.(a-c) [10f] Reproduced with permission. Copyright 2016, American Chemical Society.(d,e) [10e]Reproduced with permission. Copyright 2015, American Chemical Society.

5.3 Mo_6S_8 for Al-ion batteries

Owing to the advanced merits of the most abundant metal in the earth's crust and much higher energy density of 1060 Wh kg^{-1} than LIBs (406 Wh kg^{-1}), AIBs have

attracted more attention recently. To date, AIBs mainly suffers from its low capacity, limited rate capability, high cost of suitable electrolyte (*e.g.*,ionic liquids) and suitable cathode materials.[22c, 28] In order to search the suitable cathode candidates, the electrode with large frame structure to host the Al intercalation is critically important. This is mainly due to the strong Coulombic effect induced by the Al cation with three positive charges, leading to difficult electrochemical Al intercalation into a host crystal structure. Mo_6S_8 with a unique crystal structure and theoretical capacity of 193 mA h g^{-1} have attracted attention for its application in AIBs. Geng *et al.*[10e] fabricated a reversible electrochemical cell based on the use of Mo_6S_8 electrode and ionic liquids (IL) as the electrolyte consist of $AlCl_3$ and 1-butyl-3-methylimidazoliumchloride ((BMIm)Cl). By using a mixture of $AlCl_3$ and (BMIm)Cl with a molar ratio of 1.5:1, the reaction mechanism of Mo_6S_8 for AIBs can be simply expressed as follows:

Anode: $Al + 7(AlCl)^- \leftrightarrow 4Al_7(AlCl)^- + 3e^-$

Cathode: $4Al_7(AlCl)^- + 6e^- + Mo_6S_8 \leftrightarrow Al_2Mo_6S_8 + 14(Al\ Cl)$

As shown in **Figure 6d**, the cell displays a two-step electrochemical reaction between Mo_6S_8 and Al, as evidenced by two redox peaks and two discharge-charge plateaus. This also indicates there are two intercalation sites for Al (Al 1 and Al 2) during the insertion and extraction process (**Figure 6e**). At an extremely low current density of 2.4 mA g^{-1}, the Mo_6S_8 could deliver a capacity of 167 mAh g^{-1}, corresponding to the formation of $Al_{1.73}Mo_6S_8$. At current higher densities of 60 mA g^{-1} and 120 mA g^{-1}, the discharge capacity of Mo_6S_8 is only 40 mA h g^{-1} and 25 mAh g^{-1} , respectively, indicating a limited capacity obtained from Mo_6S_8 for AIBs.

6. Conclusion and Perspectives

Owing to the unique open crystal structures and strong electrochemical kinetics with various multivalent ions (*e.g.*, Zn^{2+}, Mg^{2+}, Mn^{2+}, Co^{2+}, Fe^{2+} and Al^{3+}), the *Chevrel* phase Mo_6T_8 (especially, T = S) have attracted increasing attention as electrode candidates for advanced batteries, including monovalent ion batteries (*e.g.*, LIBs and SIBs) and multivalent ion batteries (*e.g.*, MIBs, ZIBs and AIBs). In this Progress report, we briefly summarize recent significant progress on the *Chevrel*

phase Mo_6T_8, including various synthesis methods (*e.g.*, solid state method, molten salt method, graphene-assisted method and microwave-assisted method), ion storage properties in various metal-ion-batteries and their corresponding electrochemical mechanisms (*e.g.*, $Mo_6S_8 \leftrightarrow M_xMo_6S_8$ and charge trapping within MMo_6S_8). Despite the achieved progress,, there are still many challenges remain for the continued investigation of Mo_6T_8 for their application in batteries. First of all, the synthesis methods or conditions of Mo_6T_8, including long time in total, high temperature, high cost, limit yield, low mass production, still needs to be further optimized. Secondly, the electrochemical performance (especially, initial Coulombic efficiency, rate capability and cycling life) of Mo_6T_8 is still unsatisfied. Several strategies (*e.g.*, nano-engineering of Mo_6T_8 with diverse structures, hybridization of Mo_6T_8 with highly conductive agents and heteroatom doping Mo_6T_8) are highly welcome. In addition, to better and further understand the working mechanism of Mo_6T_8 for their applications in advanced batteries, advanced characteristic approaches (especially, *in-situ* observed technique) should be also employed, together with the corresponding theoretical calculation. Considering the short history of the research on Mo_6T_8 electrode for advanced batteries, , it is highly expected many progress can be achieved in the future.

Supporting Information

Supporting Information is available from the Wiley Online Library or from the author.

Acknowledgements

This work was supported by the National Natural Science Foundation of China (Grant Nos. 51302079) and Australia Research Council (DP160102627).

Received: ((will be filled in by the editorial staff))

Revised: ((will be filled in by the editorial staff))

Published online: ((will be filled in by the editorial staff))

References

[1] a) P. Poizot, S. Laruelle, S. Grugeon, L. Dupont, J. Tarascon, *Nature* **2000**, *407*, 496; b) K. T. Nam, D. W. Kim, P. J. Yoo, C. Y. Chiang, N. Meethong, P. T. Hammond, Y. M. Chiang, A. M. Belcher, *Science* **2006**, *312*, 885; c) H. G. Jung, M. W. Jang, J. Hassoun, Y. K. Sun, B. Scrosati, *Nat. Commun*. **2011**, *2*, 51.

[2] a) Y. S. Guo, F. Zhang, J. Yang, F. F. Wang, Y. NuLi, S. I. Hirano, *Energy Environ. Sci*. **2012**, *5*, 9100; b) S. W. Kim, D. H. Seo, X. Ma, G. Ceder, K. Kang, *Adv. Energy Mater*. **2012**, *2*, 710; c) Y. Wang, X. Yu, S. Xu, J. Bai, R. Xiao, Y. S. Hu, H. Li, X. Q. Yang, L. Chen, X. Huang, *Nat. Commun*. **2013**, *4*. 2858; d) R. C. Massé, E. Uchaker, G. Cao, *Sci. China Mater.***2015**, *58*, 715.

[3] a) M. Pasta, C. D. Wessells, R. A. Huggins, Y. Cui, *Nat. Commun*. **2012**, *3*, 1149; b) L. Suo, O. Borodin, T. Gao, M. Olguin, J. Ho, X. Fan, C. Luo, C. Wang, K. Xu, *Science* **2015**, *350*, 938; c) K. Nakamoto, Y. Kano, A. Kitajou, S. Okada, *J. Power Sources* **2016**, *327*,, 327.

[4] a) F. Zhang, T. Zhang, X. Yang, L. Zhang, K. Leng, Y. Huang, Y. Chen, *Energy Environ. Sci*. **2013**, *6*, 1623; b) Y. Cheng, L. R. Parent, Y. Shao, C. M. Wang, V. L. Sprenkle, G. Li, J. Liu, *Chem. Mater.* **2014**, *26*.

[5] a) V. Etacheri, R. Marom, R. Elazari, G. Salitra, D. Aurbach, *Energy Environ. Sci.* **2011**, *4*, 3243; b) J. B. Goodenough, K. S. Park, *J. Am. Chem. Soc.* **2013**, *135*, 1167; c) L. Lu, X. Han, J. Li, J. Hua, M. Ouyang, *J. Power Sources* **2013**, *226*, 272; d) R. Y. Wang, C. D. Wessells, R. A. Huggins, Y. Cui, *Nano Lett.* **2013**, *13*, 5748; e) J. Xu, S. Dou, H. Liu, L. Dai, *Nano Energy* **2013**, *2*, 439; f) S. Goriparti, E. Miele, F. De Angelis, E. Di Fabrizio, R. P. Zaccaria, C. Capiglia, *J. Power Sources* **2014**, *257*, 421; g) Y. Zhao, X. Li, B. Yan, D. Li, S. Lawes, X. Sun, *J. Power Sources* **2015**, *274*, 869; h) d) J. Xu, J. Ma, Adv. Mater. 2017

[6] a) X. Rui, N. Yesibolati, C. Chen, *J. Power Sources* **2011**, *196*, 2279; b) V. Aravindan, J. Gnanaraj, Y. S. Lee, S. Madhavi, *Chem. Rev.* **2014**, *114*, 11619; c) N. Nitta, F. Wu, J. T. Lee, G. Yushin, *Mater. Today* **2015**, *18*, 252; d) J. Xu, J. Ma,.. Adv. Sci.2017

[7] a) M. Levi, H. Gizbar, E. Lancry, Y. Gofer, E. Levi, D. Aurbach, *J. Electroanal. Chem.* **2004**, *569*, 211; b) D. A. Tompsett, M. S. Islam, *Chem. Mater.* **2013**, *25*, 2515; c) L. David, R. Bhandavat, G. Singh, *ACS Nano* **2014**, *8*, 1759; d) C. Cui, X. Li, Z. Hu, J. Xu, H. Liu, J. Ma, *RSC Adv.* **2015**, *5*, 92506; e) L. Yu, S. Xi, C. Wei, W. Zhang, Y. Du, Q. Yan, Z. Xu, *Adv. Energy Mater.* **2015,** *5*, 1401517; f) G. Liu, X. Liu, L. Wang, J. Ma, H. Xie, X. Ji, J. Guo, R. Zhang, *Electrochim. Acta* **2016**, *222*, 1103.

[8] a) M. M. Huie, D. C. Bock, E. S. Takeuchi, A. C. Marschilok, K. J. Takeuchi, *Coord. Chem. Rev.* **2015**, *287*, 15; b) C. Liu, Z. G. Neale, G. Cao, *Mater. Today* **2016**, *19*, 109.

[9] E. Peled, *J. Electrochem. Soc.* **1979**, *126*, 2047.

[10] a) J. Tarascon, G. Hull, P. Marsh, T. Haar, *J. Solid State Chem.* **1987**, *66*, 204; b) M. Wakihara, T. Uchida, K. Suzuki, M. Taniguchi, *Electrochim. Acta* **1989**, *34*, 867; c) E. Levi, E. Lancry, A. Mitelman, D. Aurbach, G. Ceder, D. Morgan, O. Isnard, *Chem. Mater.* **2006**, *18*, 5492; d) R. Y. Wang, C. D. Wessells, R. A. Huggins, Y. Cui, *Nano Lett.* **2013**, *13*, 5748; e) L. Geng, G. Lv, X. Xing, J. Guo, *Chem. Mater.* **2015**, *27*, 4926; f) M. S. Chae, J. W. Heo, S. C. Lim, S. T. Hong, *Inorg. Chem.* **2016**, *55*, 3294; g) B. Lee, H. R. Lee, T. Yim, J. H. Kim, J. G. Lee, K. Y. Chung, B. W. Cho, S. H. Oh, *J. Electrochem. Soc*. **2016**, *163*, A1070.

[11] D. Aurbach, Z. Lu, A. Schechter, Y. Gofer, H. Gizbar, R. Turgeman, Y. Cohen, M. Moshkovich, E. Levi, *Nature* **2000**, *407*, 724.

[12] E. Gocke, W. Schramm, P. Dolscheid, R. Scho, *J. Solid State Chem*. **1987**, *70*, 71.

[13] M. Levi, E. Lancri, E. Levi, H. Gizbar, Y. Gofer, D. Aurbach, *Solid State Ionics* **2005**, *176*, 1695.

[14] a) E. Lancry, E. Levi, Y. Gofer, M. Levi, G. Salitra, D. Aurbach, *Chem. Mater.* **2004**, *16*, 2832; b) D. Aurbach, G. S. Suresh, E. Levi, A. Mitelman, O. Mizrahi, O. Chusid, M. Brunelli, *Adv. Mater.* **2007**, *19*, 4260; c) S. G. Woo, J. Y. Yoo, W. Cho, M. S. Park, K. J. Kim, J. H. Kim, J. S. Kim, Y. J. Kim, *RSC Adv.* **2014**, *4*, 59048; d) L. Geng, G. Lv, X. Xing, J. Guo, *Chem. Mater.* **2015**, *27*, 4926; e) S. H. Choi, J. S. Kim, S. G. Woo, W. Cho, S. Y. Choi, J. Choi, K. T. Lee, M. S. Park, Y. J. Kim, *ACS Appl. Mater. Interfaces* **2015**, *7*, 7016.

[15] a) Y. V. Mironov, A. V. Virovets, N. G. Naumov, V. N. Ikorskii, V. E. Fedorov, *Chem. Eur. J.* **2000**, *6*, 1361; b) E. Lancry, E. Levi, A. Mitelman, S. Malovany, D. Aurbach, *J.Solid State Chem.* **2006**, *179*, 1879; c) A. Ryu, M. S. Park, W. Cho, J. S. Kim, Y. J. Kim, *Bull Korean Chem Soc* **2013**, *34*, 3033.

[16] a) G. Gershinsky, O. Haik, G. Salitra, J. Grinblat, E. Levi, G. D. Nessim, E. Zinigrad, D. Aurbach, *J. Solid State Chem.* **2012**, *188*, 50; b) Y. Cheng, L. R. Parent, Y. Shao, C. Wang, V. L. Sprenkle, G. Li, J. Liu, *Chem. Inform* **2014**, *45*, 4904; c) P. Saha, P. H. Jampani, M. K. Datta, C. U. Okoli, A. Manivannan, P. N. Kumta, *J. Electrochem. Soc.* **2014**, *161*, A593; d) F. Murgia, P. Antitomaso, L. Stievano, L. Monconduit, R. Berthelot, *J. Solid State Chem.* **2016**, *242*, 151; e) Y. Cheng, L. Luo, L. Zhong, J. Chen, B. Li, W. Wang, S. X. Mao, C. Wang, V. L. Sprenkle, G. Li, *ACS Appl. Mater. Interfaces* **2016**, *8*, 13673.

[17] a) J. Tarascon, J. Waszczak, G. Hull, F. DiSalvo, L. Blitzer, *Solid State Commun.* **1983**, *47*, 973; b) E. Gocke, R. Schöllhorn, G. Aselmann, W. Müller-Warmuth, *Inorg. Chem.* **1987**, *26*, 1805; c) F. Garcia- Alvarado, J. Tarascon, B. Wilkens, *J. Electrochem. Soc.* **1992**, *139*, 3206; d) L. Guohua, H. Ikuta, T. Uchida, M. Wakihara, *J. Power Sources* **1995**, *54*, 519.

[18] M. Nagao, H. Kitaura, A. Hayashi, M. Tatsumisago, *J. Electrochem. Soc.* **2013**, *160*, A819.

[19] F. Wang, Y. Lin, L. Suo, X. Fan, T. Gao, C. Yang, F. Han, Y. Qi, K. Xu, C. Wang, *Energy Environ. Sci.* **2016**, *9*, 3666.

[20] a) D. Hamani, M. Ati, J. M. Tarascon, P. Rozier, *Electrochem. Commun.* **2011**, *13*, 938; b) N. Yabuuchi, M. Kajiyama, J. Iwatate, H. Nishikawa, S. Hitomi, R. Okuyama, R. Usui, Y. Yamada, S. Komaba, *Nat. Mater.* **2012**, *11*, 512; c) V.

Palomares, P. Serras, I. Villaluenga, K. B. Hueso, J. Carretero-González, T. Rojo, *Energy Environ. Sci*. **2012**, *5*, 5884; d) J. Qian, Y. Xiong, Y. Cao, X. Ai, H. Yang, *Nano Lett.* **2014**, *14*, 1865.

[21] P. Saha, P. H. Jampani, M. K. Datta, D. Hong, C. U. Okoli, A. Manivannan, P. N. Kumta, *J. Phys. Chem. C* **2015**, *119*, 5771.

[22] a) C. Xu, B. Li, H. Du, F. Kang, *Angew. Chem. Int. Ed.* **2012**, *51*, 933; b) R. Mohtadi, F. Mizuno, Beilstein, *J. Nanotech.* **2014**, *5*, 1291; c) M. C. Lin, M. Gong, B. Lu, Y. Wu, D. Y. Wang, M. Guan, M. Angell, C. Chen, J. Yang, B. J. Hwang, *Nature* **2015**, *520*, 324; d) J. W. Choi, D. Aurbach, *Nat. Rev. Mater.* **2016**, *1*, 16013.

[23] a) B. Liu, T. Luo, G. Mu, X. Wang, D. Chen, G. Shen, *ACS Nano* **2013**, *7*, 8051; b) Y. Shao, M. Gu, X. Li, Z. Nie, P. Zuo, G. Li, T. Liu, J. Xiao, Y. Cheng, C. Wang, *Nano Lett.* **2013**, *14*, 255; c) N. Singh, T. S. Arthur, C. Ling, M. Matsui, F. Mizuno, *Chem. Commun.* **2013**, *49*, 149; d) S. Tepavcevic, Y. Liu, D. Zhou, B. Lai, J. Maser, X. Zuo, H. Chan, P. Král, C. S. Johnson, V. Stamenkovic, *ACS Nano* **2015**, *9*, 8194.

[24] A. Mitelman, E. Levi, E. Lancry, D. Aurbach, *ECS Trans.* **2007**, *3*, 109.

[25] a) E. Levi, Y. Gofer, Y. Vestfreed, E. Lancry, D. Aurbach, *Chem. Mater.* **2002**, *14*, 2767; b) A. Mitelman, M. Levi, E. Lancry, E. Levi, D. Aurbach, *Chem. Commun.* **2007**, *41*, 4212.

[26] a) Y. Li, H. Dai, *Chem. Soc. Rev.* **2014**, *43*, 5257; b) M. H. Alfaruqi, V. Mathew, J. Gim, S. Kim, J. Song, J. P. Baboo, S. H. Choi, J. Kim, *Chem. Mater.* **2015**, *27*, 3609; c) D. Kundu, B. D. Adams, V. Duffort, S. H. Vajargah, L. F. Nazar, Nature Energy 2016, 1, 16119; d) G. Li, Z. Yang, Y. Jiang, C. Jin, W. Huang, X. Ding, Y. Huang, *Nano Energy* **2016**, *25*, 211.

[27] a) R. Schöllhorn, M. Kümpers, J. Besenhard, *Mater. Res. Bulletin* **1977**, *12*, 781; b) E. Levi, G. Gershinsky, D. Aurbach, O. Isnard, *Inorg. Chem.* **2009**, *48*, 8751.

[28] a) N. Jayaprakash, S. K. Das, L. A. Archer, *Chem. Commun.* **2011**, *47*, 12610; b) D. Y. Wang, C. Y. Wei, M. C. Lin, C. J. Pan, H. L. Chou, H. A. Chen, M. Gong, Y. Wu, C. Yuan, M. Angell, *Nat. Commun.* **2017**, *8*. 14283.

Table of Contents

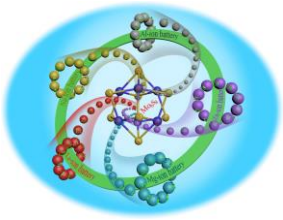

In this **Progress Reports**, we mainly overview recent progress of ***Chevrel* phase Mo_6T_8 (T= S, Se)** for their applications in monovalent (lithium and sodium) and multivalent (magnesium, zinc and aluminum) ion batteries, including synthesis methods, intercalation mechanism and various structure-function of Mo_6T_8, as well as their applications in various advanced batteries.

Corresponding author's short summary

Jianmin Ma is an associate professor in Hunan University, China. He received his B.Sc. degree in Chemistry from Shanxi Normal University in 2003 and Ph.D. degree in Materials Physics and Chemistry from Nankai University in 2011. During 2011-2015, he also conducted the research in several oversea universities as a postdoctoral research associate. His research interest focuses on the synthesis of nanostructured materials, electrochemical storage devices, electrocatalysis, and gas sensors.